

A Masked Image Reconstruction Network for Document-level Relation Extraction

Liang Zhang¹ Yidong Cheng¹

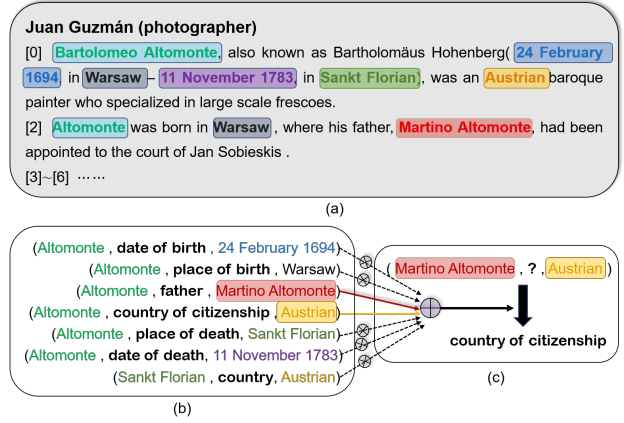
¹ Department of Artificial Intelligence, School of Informatics, Xiamen University
 {lzhang, ydcheng}@stu.xmu.edu.cn

Abstract

Document-level relation extraction aims to extract relations among entities within a document. Compared with its sentence-level counterpart, Document-level relation extraction requires inference over multiple sentences to extract complex relational triples. Previous research normally complete reasoning through information propagation on the mention-level or entity-level document-graphs, regardless of the correlations between the relationships. In this paper, we propose a novel Document-level Relation Extraction model based on a Masked Image Reconstruction network (**DRE-MIR**), which models inference as a masked image reconstruction problem to capture the correlations between relationships. Specifically, we first leverage an encoder module to get the features of entities and construct the entity-pair matrix based on the features. After that, we look on the entity-pair matrix as an image and then randomly mask it and restore it through an inference module to capture the correlations between the relationships. We evaluate our model on three public document-level relation extraction datasets, i.e. DocRED, CDR, and GDA. Experimental results demonstrate that our model achieves state-of-the-art performance on these three datasets and has excellent robustness against the noises during the inference process.

1 Introduction

Relation extraction (RE) aims to identify the semantic relations between entities from raw texts, which is of great importance to many real-world applications [Qiu *et al.*, 2019; Zhang *et al.*, 2021c; Zhang *et al.*, 2021b]. Previous researches focused on sentence-level RE, which predicts the relationship between entities in a single sentence [Zeng *et al.*, 2015; Zhang *et al.*, 2018; Baldini Soares *et al.*, 2019]. However, large amounts of relationships are expressed by multiple sentences in real life [Yao *et al.*, 2019; Verga *et al.*, 2018]. Therefore, many recent works have made efforts to extend sentence-level RE to document-level RE [Yao *et al.*, 2019; Zeng *et al.*, 2020; Zhou *et al.*, 2021b; Xu *et al.*, 2021a; Zhang *et al.*, 2021a].



Compared with sentence-level RE where a sentence contains only one entity pair to be classified, document-level RE requires the model to classify the relations of multiple entity pairs simultaneously and the entities involved in a relationship may appear in different sentences. Besides, the document-level RE also poses a great challenge, i.e. relation inference. As shown in Figure 1, it is easy to identify the intra-sentence relations shown in Figure 1b, such as $(Altomonte, date of birth, 24 February 1694)$, $(Altomonte, father, Martino Altomonte)$, and $(Altomonte, country of citizenship, Austrian)$, owing to two related entities appear in the same sentence. However, it is more challenging for a model to predict the inter-sentential relations between *Martino Altomonte* and *Austrian* because the document does not explicitly express the relationship between them. This type of inter-sentential relations can only be identified through reasoning techniques. According to the statistics of the DocRED [Yao *et al.*, 2019] dataset which is a well-known document-level RE dataset, Most of the relation instances (61.1%) require reasoning to be identified in document-level RE, which indicates that reasoning is essential for the document-level RE.

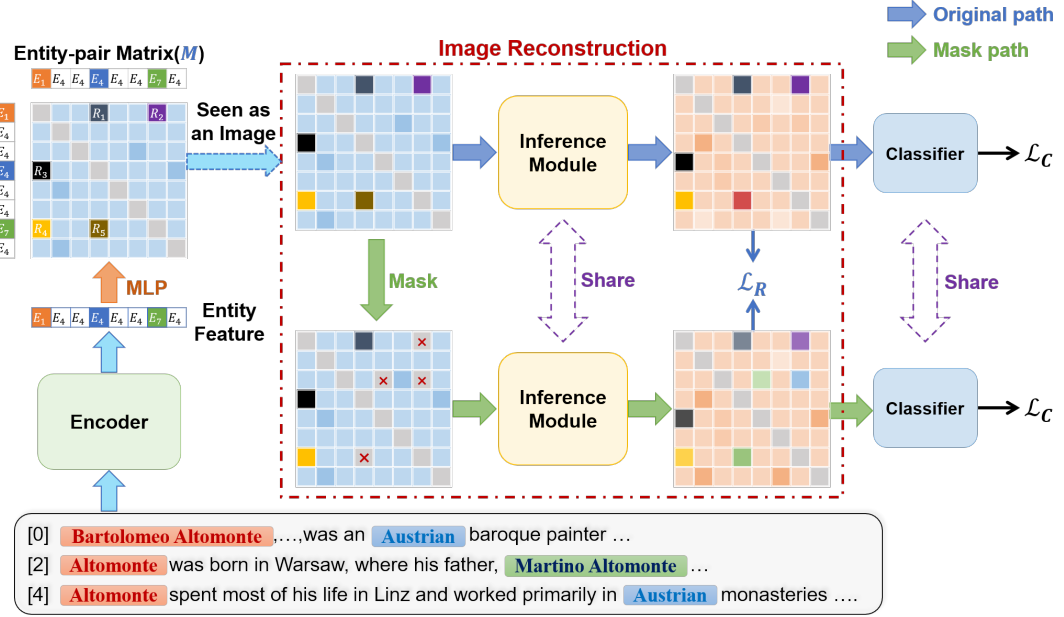


Figure 2: The overall architecture of our DRE-MIR model. Firstly, the Encoder encodes the input document to obtain the entities embedding (E_s, E_o), and then we obtain the Entity-pair Matrix M through the linear layer. Secondly, we treat the entity-pair matrix M as an image, and then randomly mask it and restore it through an inference module. Through the Masked Image Reconstruction (MIR) task, our inference module can learn how to use the correlation between relationships to infer the masked relationship. Moreover, the MIR task contains two paths, i.e. the Original path and the Mask path. Finally, we utilize a classifier to predict the relationship of each entity pair. \mathcal{L}_R and \mathcal{L}_C represent reconstruction loss and classification loss, respectively.

To extract such complex inter-sentence relations, most current approaches constructed a document-level graph based on heuristics, structured attention, or dependency structures [Zeng *et al.*, 2020; Nan *et al.*, 2020; Christopoulou *et al.*, 2019; Wang *et al.*, 2020], and then perform inference with graph convolutional network (GCN) [Guo *et al.*, 2019; Kipf and Welling, 2016] on the document-level graph. It should be noted that methods of this type complete reasoning through the information transferring between mentions or entities. Meanwhile, considering the transformer architecture can implicitly model long-distance dependencies and can be regarded as a token-level fully connected graph, some studies [Tang *et al.*, 2020; Zhou *et al.*, 2021b] implicitly infers through the pre-trained model rather than via the document-level graphs.

However, these methods ignore the correlation between relationships. As shown in Figure 1, we can easily infer the inter-sentence relation (*Martino Altomonte, country of citizenship, Austrian*) through the correlation between the relationships. Specifically, the model needs to firstly capture the correlation among (*Altomonte, father, Martino Altomonte*), (*Altomonte, country of citizenship, Austrian*), and (*Martino Altomonte, country of citizenship, Austrian*), and then use reasoning techniques to identify this complex inter-sentential relation as shown in Figure 1c.

To capture the interdependencies among the multiple relationships, DocuNet [Zhang *et al.*, 2021a] formulates the document-level RE as a semantic segmentation problem and uses a U-shaped segmentation module over the image-style feature map to capture global interdependencies among triples.

The DocuNet model has achieved the latest state-of-the-art performance, which shows that the correlation between relationships is essential for the document-level RE. However, capturing correlations between relations through convolutional neural networks is unintuitive and inefficient due to the intrinsic distinction between entity-pair matrices and image.

In this paper, we followed the DocuNet and model the document-level RE as a table filling problem. We first construct an entity-pair matrix, where each point represents the relevant feature of an entity pair. Then, the document-level RE model labels each point of the entity-pair matrix with the corresponding relationships class. Meanwhile, we also treat the entity-pair matrix as an image. To more effectively capture the interdependencies among the relations, we propose a novel **Document-level Relation Extraction** model based on a **Masked Image Reconstruction** network (**DRE-MIR**), which formulates the inference problem in document-level RE as a masked image reconstruction problem. As shown in Figure 2, we first randomly mask the entity-pair matrix, and then reconstruct the entity pair matrix through the inference model. Through this the Masked Image Reconstruction (**MIR**) task, our model can learn how to infer masked points with the help of correlations between relations. Moreover, to more efficiently and intuitively reconstruct the masked points in the entity-pair matrix, we propose an Inference Multi-head Self-Attention (**I-MSA**) module which can greatly improve the inference ability of the model. As shown in Figure 3, the I-MSA contains four heads and each head corresponds to an inference mode including: $\mathbf{A} \rightarrow * + * \rightarrow \mathbf{B} \implies \mathbf{A} \rightarrow \mathbf{B}$, $\mathbf{A} \rightarrow *$

$$+ \mathbf{B} \rightarrow * \implies \mathbf{A} \rightarrow \mathbf{B}, * \rightarrow \mathbf{A} + \mathbf{B} \rightarrow * \implies \mathbf{A} \rightarrow \mathbf{B}, \text{ and } * \rightarrow \mathbf{A} + * \rightarrow \mathbf{B} \implies \mathbf{A} \rightarrow \mathbf{B}.$$

Our contributions can be summarized as follows:

- To the best of our knowledge, our method is the first approach that treat the inference problem in document-level RE as an image reconstruction problem.
- We introduce the I-MSA to improve the model's ability to reconstruct the masked entity-pair matrix.
- Experimental results on three public document-level RE datasets shows that our Dense-CCNet model can achieve state-of-the-art performance.

2 Method

In this section, we introduce in detail our DRE-MIR model. As shown in Figure 2, the DRE-MIR mainly consists of 3 modules, i.e. encoder module, inference module, and classifier module. We first describe the encoder module in Section 2.1, then introduce the core module, i.e. inference module, in Section 2.2, finally we describe our classifier module and loss function in Section 2.3.

2.1 Encoder Module

[Zhong and Chen, 2020] and [Zhou and Chen, 2021] verified that marking entities in the input sentence by entity type can effectively improve the performance of sentence-level RE model. However, in document-level RE, each entity has multiple mentions and it is important to gather all the mention information for each entity. Therefore, we use the entity type and entity id to mark the mentions in the document, which not only can incorporate the entity type information earlier but also help to improve the aggregation of the mention information. Specifically, given document $D = \{w_i\}_{i=1}^l$ containing l words, we first mark the mention in the document by inserting special symbols $\langle e_t \rangle$ and $\langle e_{id} \rangle$ at the start and end position of the mentions, where e_t and e_{id} respectively represent the entity type and entity id of the mention. Then we feed the adapted document to the pre-trained language model to obtain the context embedding of each word in the document:

$$H = [h_1, \dots, h_l] = \text{Encoder}([w_1, \dots, w_l]). \quad (1)$$

Finally, we utilize the average of the embeddings of $\langle e_t \rangle$ and $\langle e_{id} \rangle$ to represent the mention.

For an entity e_i with mentions $\{m_j^i\}_{j=1}^{N_{e_i}}$, we follow [Zhou *et al.*, 2021b] and [Zhang *et al.*, 2021a], and leverage logsumexp pooling [Jia *et al.*, 2019], a smooth version of max pooling, to obtain the embedding h_{e_i} of entity e_i :

$$h_{e_i} = \log \sum_{j=1}^{N_{e_i}} \exp(h_{m_j^i}). \quad (2)$$

In addition, we calculate an entity-pair-aware context representation $c_{s,o}$ for each entity pair (e_s, e_o) , which represents the contextual information in the document that the entity e_s and the entity e_o together pay attention to. The $c_{s,o}$ is formulated as:

$$\begin{aligned} c_{s,o} &= Ha_{s,o}, \\ a_{s,o} &= \text{softmax}(A_s * A_o), \end{aligned} \quad (3)$$

where $A_s (A_o)$ refers to the attention score that entity $e_s (e_o)$ pays attention to each word in the document, H is the document embedding, and $*$ refers to element-wise multiplication.

Finally, we construct an entity-pair matrix $M \in \mathbb{R}^{N_e \times N_e \times d}$ as follows:

$$\begin{aligned} M_{s,o} &= \text{FFN}([u_s, u_o]), \\ u_s &= W_s[h_{e_s}, h_{\text{doc}}, c_{s,o}], \\ u_o &= W_o[h_{e_o}, h_{\text{doc}}, c_{s,o}], \end{aligned} \quad (4)$$

where N_e represents the number of entities, $\text{FFN}()$ refers to a feed-forward neural network, W_s and W_o are the learnable weight matrix, h_{doc} is [CLS] token embedding which is used to represent the information of the entire document.

2.2 Inference Module

After getting the entity-pair matrix, we treat it as an image. We obtain a masked image by randomly masking the pixels of the original image and reconstruct the masked image through an inference module, as shown in Figure 2. Through this the Masked Image Reconstruction (**MIR**) task, our inference module can learn how to infer the masked pixels from the unmasked pixels by the correlation between the relationships.

Our inference module is a variant of Transformer's encoder, which replaces Multi-head Self-Attention (MSA) with Inference Multi-head Self-Attention (I-MSA), as shown in Figure 3. The I-MSA contains four heads and each head corresponds to an inference mode including: $\mathbf{A} \rightarrow *$ $+ * \rightarrow \mathbf{B} \implies \mathbf{A} \rightarrow \mathbf{B}$, $\mathbf{A} \rightarrow * + \mathbf{B} \rightarrow * \implies \mathbf{A} \rightarrow \mathbf{B}$, $* \rightarrow \mathbf{A} + \mathbf{B} \rightarrow * \implies \mathbf{A} \rightarrow \mathbf{B}$, and $* \rightarrow \mathbf{A} + * \rightarrow \mathbf{B} \implies \mathbf{A} \rightarrow \mathbf{B}$. For example, for head 1 in Figure 3 which corresponds to $\mathbf{A} \rightarrow *$ $+ * \rightarrow \mathbf{B} \implies \mathbf{A} \rightarrow \mathbf{B}$ inference mode, we first concatenate the corresponding pixels in the A -th row and B -th column of the image, $\{[M_{A \rightarrow 1}^1, M_{1 \rightarrow B}^1], \dots, [M_{A \rightarrow N}^1, M_{N \rightarrow B}^1]\}$, and perform dimensionality reduction through a linear layer, $\{M_{A \rightarrow 1 \rightarrow B}^1, \dots, M_{A \rightarrow N \rightarrow B}^1\}$. Then, $M_{A,B}^1$ performs an attention operation on $\{M_{A \rightarrow 1 \rightarrow B}^1, \dots, M_{A \rightarrow N \rightarrow B}^1; M_{A,B}^1\}$. The whole process can be formulated as follows:

$$\begin{aligned} M_{A,B}^1 &= \text{Attention}(M_{A,B}^1 W^Q, M_{inf}^1 W^K, M_{inf}^1 W^V), \\ M_{inf}^1 &= \{M_{A \rightarrow 1 \rightarrow B}^1, \dots, M_{A \rightarrow N \rightarrow B}^1; M_{A,B}^1\}, \\ M_{A \rightarrow * \rightarrow B}^1 &= \text{Liner}([M_{A \rightarrow *}, M_{* \rightarrow B}^1]), \end{aligned}$$

where, $[]$ represents the concatenation operation, $\{ \}$ refers to a set, W^Q, W^K, W^V are the learnable weight matrix.

Inspired by [Bao *et al.*, 2021] and [Zhou *et al.*, 2021a], we reconstruct the distribution of the pixels of the masked image on the label, $p(r|M_{A,B})$, instead of reconstructing the raw pixels, $M_{A,B}$. The reason is that labels are more information-dense than pixels and $p(r|M_{A,B})$ is closer to our target task, relation classification. In addition, we reconstruct each pixel on the masked image including the masked pixel and the unmasked pixel, which is similar to the [He *et al.*, 2021] method. In this way, the convergence of the model can be accelerated and better performance can be obtained. Specifically, the original image M_o and the masked image M_m are first sequentially input to the inference module and the classifier module to obtain the probability distributions $p(r|M_o)$ and $p(r|M_m)$. Then, we reconstruct the masked image by minimizing bidirectional

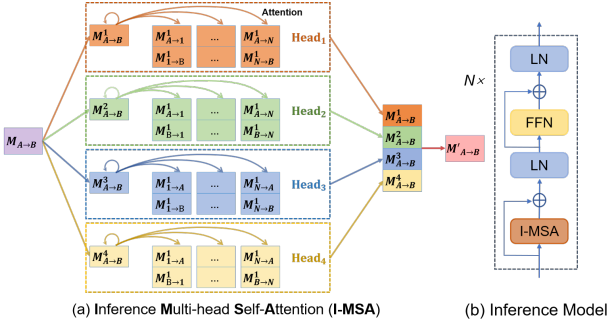


Figure 3: (a) The architecture of the Inference Multi-head Self-Attention (I-MSA), which is a variant of multi-head self-attention (MSA). The I-MSA has four types of heads and each head corresponds to one inference mode. (b) Inference module, which is a variant of Transformer’s encoder by replacing MSA with I-MSA.

KL-divergence between the two distributions of corresponding pixels in the original image and masked image. Finally, our reconstruction loss function L_R is formulated as follows:

$$L_R = \frac{1}{2} \cdot (D_{KL}(p(r|M_o) \| p(r|M_m)) + D_{KL}(p(r|M_m) \| p(r|M_o))). \quad (5)$$

2.3 Classifier Module

Our classifier module is a single linear layer. The original image M_o and the masked image M_m are respectively input to the inference module to obtain the corresponding corrected image, M'_o and M'_m . Then, the relation probability of each entity pair is obtained through a linear layer:

$$P(r|M'_*) = \sigma(W_r M'_*), \quad (6)$$

$$M'_* = \text{Inference}(M_*),$$

where $*$ $\in \{o, m\}$, and W_r is model parameters.

To alleviate the problem of unbalanced relationship distribution, we use adaptive-thresholding loss [Zhou *et al.*, 2021b] as our classification loss function L_C , which learns an adaptive threshold for each sample. Specifically, a TH class is introduced to separate positive classes and negative classes: positive classes would have higher probabilities than TH , and negative classes would have lower probabilities than TH . The adaptive-thresholding loss is formulated as follows:

$$L_C = L_1 + L_2, \quad (7)$$

$$L_1 = - \sum_{r \in P_D} \log \left(\frac{\exp(\text{logit}_r)}{\sum_{r' \in \{P_D, TH\}} \exp(\text{logit}_{r'})} \right),$$

$$L_2 = - \log \left(\frac{\exp(\text{logit}_{TH})}{\sum_{r' \in \{N_D, TH\}} \exp(\text{logit}_{r'})} \right),$$

where P_D and N_D are the positive classes set and negative classes set respectively.

The training objective is to minimize the loss function L , which is defined as follows:

$$L = \alpha L_R + \beta L_C$$

α and β are hyperparameters and we simply set them to 1.

3 Experiments

3.1 Datasets

We conduct experiments on three document-level RE datasets to evaluate our DRE-MIR model. The statistics of the datasets could be found in Appendix A.

- **DocRED** [Yao *et al.*, 2019]: DocRED is a large-scale human-annotated dataset for document-level RE, which is constructed from Wikipedia and Wikidata. DocRED contains 96 types of relations, 132,275 entities, and 56,354 relationship triples in total. In DocRED, more than 40.7% of relational facts can only be extracted from multiple sentences, and 61.1% of relational triples require various reasoning skills. We follow the standard split of the dataset, 3,053 documents for training, 1,000 for development and, 1,000 for the test.
- **CDR** [Li *et al.*, 2016]: The Chemical-Disease Reactions dataset (CDR) consists of 1,500 PubMed abstracts, which is equally divided into three sets for training, development, and testing. CDR is aimed to predict the binary interactions between Chemical and Disease concepts.
- **GDA** [Wu *et al.*, 2019]: The Gene-Disease Associations dataset (GDA) is a large-scale biomedical dataset, which is constructed from MEDLINE abstracts by method of distant supervision. GDA contains 29,192 documents as the training set and 1,000 as the test set. GDA is also a binary relation classification task that identifies Gene and Disease concepts interactions. We follow [Christopoulou *et al.*, 2019] to divide the training set into two parts, 23,353 documents for training and 5,839 for validation.

3.2 Experimental Settings

Our model was implemented based on PyTorch and Huggingface’s Trans-formers [Wolf *et al.*, 2019]. We used cased BERT-base [Devlin *et al.*, 2018] as the encoder on DocRED and SciBERT-base [Beltagy *et al.*, 2019] on CDR and GDA. Our model is optimized with AdamW [Loshchilov and Hutter, 2017] with a linear warmup [Goyal *et al.*, 2017] for the first 6% steps followed by a linear decay to 0. By default, we randomly mask 20% of points in the entity-pair matrix and set the number of layers in the inference module to 3. All hyper-parameters are tuned on the development set, some of which are listed in Appendix B.

3.3 Results on the DocRED Dataset

On the DocRED Dataset, we choose the following two types of models as the baseline:

- **Graph-based Models**: This type of method uses graph convolutional networks (GCN) [Kipf and Welling, 2016; Veličković *et al.*, 2017; Schlichtkrull *et al.*, 2018] to complete inference on document-level graphs, including GEDA [Li *et al.*, 2020], LSR [Nan *et al.*, 2020], GLRE [Wang *et al.*, 2020], GAIN [Zeng *et al.*, 2020], and Het-erGSAN [Xu *et al.*, 2021b].
- **Transformer-based Models**: These models directly use pre-trained language models for document-level RE without using graph structures, including BERT [Xu *et al.*,

Model	IgnF ₁	F ₁	Dev		Test	
			Intra-F ₁	Inter-F ₁	IgnF ₁	F ₁
GEDA-BERT _{base} [Li <i>et al.</i> , 2020]	54.52	56.16	-	-	53.71	55.74
LSR-BERT _{base} [Nan <i>et al.</i> , 2020]	52.43	59.00	65.26	52.05	56.97	59.05
GLRE-BERT _{base} [Wang <i>et al.</i> , 2020]	-	-	-	-	55.40	57.40
HeterGSAN-BERT _{base} [Zeng <i>et al.</i> , 2020]	58.13	60.18	-	-	57.12	59.45
GAIN-BERT _{base} [Xu <i>et al.</i> , 2021b]	59.14	61.22	67.10	53.90	59.00	61.24
BERT _{base} [Wang <i>et al.</i> , 2019]	-	54.16	61.61	47.15	-	53.20
BERT-TS _{base} [Wang <i>et al.</i> , 2019]	-	54.42	61.80	47.28	-	53.92
HIN-BERT _{base} [Tang <i>et al.</i> , 2020]	54.29	56.31	-	-	53.7	55.60
CorefBERT _{base} [Ye <i>et al.</i> , 2020]	55.32	57.51	-	-	54.54	56.96
ATLOP-BERT _{base} [Zhou <i>et al.</i> , 2021b]	59.22	61.09	-	-	59.31	61.30
SIRE-BERT [Zeng <i>et al.</i> , 2021]	59.82	61.60	68.07	54.01	60.18	62.05
DocuNet-BERT _{base} [Zhang <i>et al.</i> , 2021a]	59.86	61.83	-	-	59.93	61.86
DRE-MIR-BERT _{base}	60.97±0.10	62.96±0.17	68.13±0.14	57.29±0.43	61.03	63.15

Table 1: Results (%) on the development and test set of the DocRED. The scores of all the baseline models come from ATLOP [Zhou *et al.*, 2021b] and SIRE [Zeng *et al.*, 2021]. And, the results on the test set are obtained by submitting to the official Codalab.

Model	CDR	GDA
BRAN [Verga <i>et al.</i> , 2018]	62.1	-
EoG [Christopoulou <i>et al.</i> , 2019]	63.6	81.5
LSR [Nan <i>et al.</i> , 2020]	64.8	82.2
DHGI [Zhang <i>et al.</i> , 2020]	65.9	83.1
GLRE [Wang <i>et al.</i> , 2020]	68.5	-
SciBERT [Beltagy <i>et al.</i> , 2019]	65.1	82.5
ATLOP-SciBERT [Zhou <i>et al.</i> , 2021b]	69.4	83.9
DocuNet-SciBERT [Zhang <i>et al.</i> , 2021a]	76.3	85.3
DRE-MIR-SciBERT	76.6	86.4

Table 2: Results (%) on the biomedical datasets CDR and GDA.

2021b], BERT-Two-Step [Wang *et al.*, 2019], HIN-BERT [Tang *et al.*, 2020], CorefBERT [Ye *et al.*, 2020], and ATLOP-BERT [Zhou *et al.*, 2021b].

In addition, we also consider the DocuNet [Zhang *et al.*, 2021a] and SIRE [Zeng *et al.*, 2021] in the comparison. The DocuNet formulates document-level RE as a semantic segmentation problem and get the latest SOTA results. While, the SIRE represents intra- and inter-sentential relations in different ways, and design a new form of logical reasoning.

We follow [Yao *et al.*, 2019] and use F_1 and $\text{Ign}F_1$ as evaluation metrics to evaluate the performance of a model, where $\text{Ign}F_1$ denotes the F_1 score excluding the relational facts that are shared by the training and dev/test sets. Comparing all baseline model, our DRE-MIR model outperforms the latest state-of-the-art models by **1.14/1.11** $F_1/\text{Ign}F_1$ on the dev set and **1.29/1.1** $F_1/\text{Ign}F_1$ on the test set. This demonstrates that our model has an excellent overall performance. Besides, comparing the graph-based state-of-the-art model, the DRE-MIR model outperforms the GAIN model by **1.74/1.83** $F_1/\text{Ign}F_1$ on the dev set and **2.11/2.03** $F_1/\text{Ign}F_1$ on the test set. This shows that our model has better reasoning ability than the previous graph-based models.

Model	IgnF ₁	F ₁
DRE-MIR	60.97	62.96
Only Mask path	60.13	62.20
Only reconstitution masked point	59.50	61.53
w/o MIR	59.31	61.35
w/o Inference Model	58.56	60.46
w/o I-MSA	54.67	56.22

Table 3: Ablation study of the DRE-MIR model on the development set of the DocRED. **w/o Inference Model** and **w/o MIR** removes the Inference Model and the MIR task from our mode, respectively; **w/o I-MSA** replaces the Inference Multi-head Self-Attention (I-MSA) with the multi-head self-attention (MSA); **w/o Inference Model** is our base model.

The same as [Nan *et al.*, 2020; Xu *et al.*, 2021b], we report Intra- F_1 / Inter- F_1 scores in Table 1, which only consider either intra- or inter-sentence relations respectively. Compared with Intra- F_1 , Inter- F_1 can better reflect the reasoning ability of the model. we can observe that our DRE-MIR model improved the Inter- F_1 score by **3.28** compared with the SIRE model. The improvement on Inter- F_1 demonstrates that our MIR task and Inference module can greatly improve the inference ability of the model. Moreover, the improvement on Inter- F_1 is greater than on intra- F_1 , which shows that the performance improvement of DRE-MIR is mainly contributed by the improvement of inter-sentence relations.

3.4 Results on the Biomedical Datasets

On the two biomedical datasets, CDR and GDA, we compared our model with a large number of baseline models and recent state-of-the-art models including BRAN [Verga *et al.*, 2018], EoG [Christopoulou *et al.*, 2019], LSR [Nan *et al.*, 2020], DHG [Zhang *et al.*, 2020], GLRE [Wang *et al.*, 2020], SciBERT [Beltagy *et al.*, 2019], ATLOP [Zhou *et al.*, 2021b], and DocuNet [Zhang *et al.*, 2021a].

Experiment results on two biomedical datasets are shown

Layer-number	$\text{Ign}F_1$	F_1
1-Layer	59.83	61.68
2-Layer	60.62	62.75
3-Layer	60.97	62.96

Table 4: Performance of DRE-MIR with different numbers of layers in the inference module on the development set of DocRED.

in Table 2. Our DRE-MIR model achieves **76.9** F_1 on the CDR dataset, which slightly out performs the DocuNe model by **0.3** F_1 . There are three possible reasons: (1) The CDR contains only two types of relations, which indicates that the correlation between relations is weak. (2) The CDR dataset contains very few annotated samples, making it difficult for our model to learn the underlying correlations. (3) The samples in the CDR dataset contain few entities, which leads to a small entity pair matrix and weakens the effectiveness of our MIR task. Although the GDA dataset also has problems (1) and (3), it is a large-scale corpus and contains a large number of samples. Therefore our model achieves **86.4** F_1 score on the GDA dataset, which improves **1.1** F_1 compared with the DocuNe model. Since the MIR task is a pre-training task in the field of machine vision, more data is required to obtain better performance.

3.5 Ablation Study

We conducted an ablation experiment to validate the effectiveness of different components of our DRE-MIR model on the development set of the DocRED dataset. The results are listed in Table 3.

The **w/o MIR** removes the MIR task from our model and only contains the original path in the DRE-MIR model. The **w/o MIR** achieves an F_1 score of 61.35, which outperforms the **w/o Inference Model**, our base model, by **0.99** F_1 . This shows that our inference module has a certain inference ability even without the MIR task. However, the DRE-MIR model without the MIR task (**w/o MIR**) has a performance drop of **1.61** F_1 , which proves that the MIR task can well improve the inference ability of our inference module.

The **Only Mask path** removes the original path from our model and only contains the Mask path. The **Only Mask path** is a variant of the DRE-MIR model, and its image reconstruction method is similar to [Bao *et al.*, 2021]. The **Only Mask path** leads to a drop of **0.76** F_1 in performance, which proves that the original image played a guiding role in the reconstruction process of the masked image to further improve the performance of the model.

As can be seen from **w/o I-MSA**, replacing the I-MSA with the MSA resulted in a huge performance drop of **6.74** F_1 . This shows that our I-MSA can greatly improve the inference ability of the Transformer. We also introduce an experiment where only the masked pixels are reconstructed, i.e. **Only reconstitution masked point**, and observe a performance drop of **1.43** F_1 . The possible reason is that the masked pixels may affect the unmasked pixels through our inference module, but reconstructing all the pixels can effectively alleviate this negative impact.

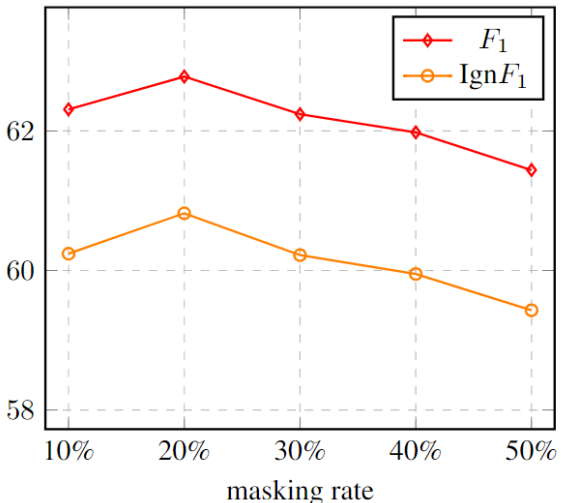


Figure 4: Results of different masking rates used in the training process on the development set of DocRED.

Overall, our model improves our base model by **2.5** F_1 , which fully demonstrates that our inference module and MIR task can effectively improve the inference ability of the model.

3.6 Analysis & Discussion

In this section, we will further discuss and analyze our DRE-MIR model from four aspects: (1) the number of layers in the inference module, (2) the masking rate during training, (3) the inference performance, and (4) the performance to restore the masked entity-pair matrix.

Table 4 shows the performance of the DRE-MIR model with different number of layers of inference modules. We observe that increasing the number of layers from 1 to 2 improves the model performance by **1.07** F_1 score. The possible reason is that increasing the number of layers can improve the multi-hop reasoning ability of the model. However, the performance of the model is slightly improved by **0.21** F_1 when the number of layers is increased from 2 to 3. Therefore, a two-layer inference module is sufficient for general cases.

Figure 4 shows that our model obtains the best performance when trained with a masking rate of 20%. However, our model still achieves a decent performance of **61.44/59.43** $F_1/\text{Ign}F_1$ when setting the masking rate to 50%, which shows that our inference module has strong inference ability to restore the masked entity-pair matrix. This also implies that using a larger masking rate to increase the training difficulty should achieve better performance under large-scale corpora, which is similar to the conclusions drawn from pre-training tasks in machine vision, such as MAE [He *et al.*, 2021].

To evaluate the inference ability of the models, we follow [Xu *et al.*, 2021b; Zeng *et al.*, 2021] and report Infer- F_1 scores in table 5, which only considers relations that engaged in the relational reasoning process. We observe that our DRE-MIR model improves **2.71** Infer- F_1 compared with the GAIN model. Removing the inference module from our model results in a performance drop of **4.10** Infer- F_1 , which demonstrates that our inference module and the MIR task can improve the

Model	Infer- F_1	P	R
GAIN-GloVe	40.82	32.76	54.14
SIRE-GloVe	42.72	34.83	55.22
BERT-RE _{base}	39.62	34.12	47.23
RoBERTa-RE _{base}	41.78	37.97	46.45
GAIN-BERT _{base}	46.89	38.71	59.45
DRE-MIR-BERT _{base}	49.60	42.72	59.13
w/o Inference Model	45.50	38.03	56.63

Table 5: Infer- F_1 results of the DRE-MIR model on the development set of DocRED. P: Precision, R: Recall.

inference ability of the model.

To evaluate the model’s ability of restoring the masked entity-pair matrix, we also randomly mask the entity-pair matrix during validating. We show the experimental results in Figure 5. Since we train our model with a masking rate of 20%, the performance drop of the model is very slight when the masking rate is less than 20%. Our model has only a slight performance drop of **1.84/1.88** F_1 /Ign F_1 with 50% masking rate, which shows that our model has excellent robustness. Even if the masking rate is increased to 80%, our model still achieves a score of **55.00/52.69** F_1 /Ign F_1 , which is better than the BERT-TS_{base} [Wang *et al.*, 2019] model. This shows that our model has strong restoring ability.

4 Related Work

Since many relational facts in real applications can only be recognized across sentences, a lot of recent work gradually shift their attention to document-level RE. Due to graph neural network(GNN) can effectively model long-distance dependence and complete logical reasoning, Many methods based on document-graphs are widely used for document-level RE. Specifically, they first constructed a graph structure from the document, and then applied the GCN [Kipf and Welling, 2016; Huang *et al.*, 2017] to the graph to complete logical reasoning. The graph-based method was first introduced by [Quirk and Poon, 2016] and has recently been extended by many works [Christopoulou *et al.*, 2019; Li *et al.*, 2020; Zhang *et al.*, 2020; Zhou *et al.*, 2020; Wang *et al.*, 2020; Nan *et al.*, 2020; Zeng *et al.*, 2020; Wu *et al.*, 2019]. [Li *et al.*, 2020] proposed the Graph Enhanced Dual Attention network (GEDA) model and used it to characterize the complex interaction between sentences and potential relation instances. [Zeng *et al.*, 2020] propose Graph Aggregation-and-Inference Network (GAIN) model. GAIN first constructs a heterogeneous mention-level graph (hMG) to model complex interaction among different mentions across the document and then constructs an entity-level graph (EG), finally uses the path reasoning mechanism to infer relations between entities on EG. [Nan *et al.*, 2020] proposed a novel LSR model, which constructs a latent document-level graph and completes logical reasoning on the graph.

In addition, due to the pre-trained language model based on the transformer architecture can implicitly model long-distance dependence and complete logical reasoning, some studies [Tang *et al.*, 2020; Zhou *et al.*, 2021b; Wang *et al.*,

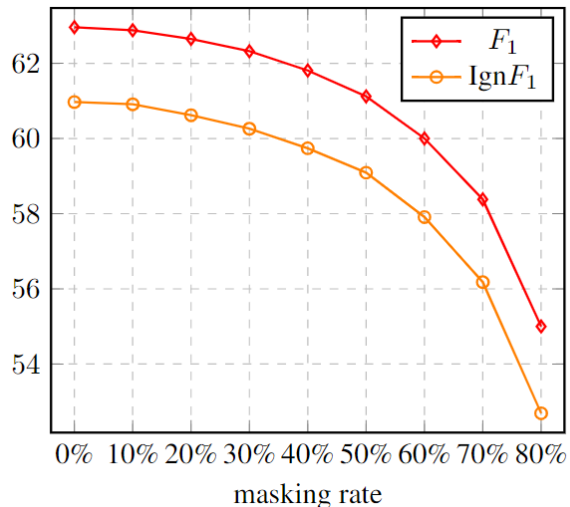


Figure 5: Results of different masking rates used the validating process on the development set of DocRED.

2019] directly apply pre-trained model without introducing document graphs. [Zhou *et al.*, 2021b] proposed an ATLOP model that consists of two parts: adaptive thresholding and localized context pooling, to solve the multi-label and multi-entity problems. The SIRE [Zeng *et al.*, 2021] represents intra- and inter-sentential relations in different ways, and design a new and straightforward form of logical reasoning. Recently, the state-of-the-ar model, DocuNet [Zhang *et al.*, 2021a], formulates document-level RE as semantic segmentation task and capture global information among relational triples through the U-shaped segmentation module [Ronneberger *et al.*, 2015].

Furthermore, our work is inspired by recent pre-training research in the field of machine vision, such as BIET [Bao *et al.*, 2021], IBOT [Zhou *et al.*, 2021a], and MAE [He *et al.*, 2021]. BEIT followed BERT [Devlin *et al.*, 2018] and proposed a masked image modeling (MIM) task and a tokenizer to pre-train vision Transformers. The tokenizer “tokenize” the image to discrete visual tokens, which is obtained by the latent codes of discrete VAE [Ramesh *et al.*, 2021]. The IBOT can perform the MIM task with an online tokenizer and formulates the MIM task as knowledge distillation (KD) distillation problem. The MAE develops an asymmetric encoder-decoder architecture, with an encoder that operates only on the visible subset of patches (without mask tokens), along with a lightweight decoder that reconstructs the original image from the latent representation and mask tokens.

5 Conclusion and Future Work

In this work, We first formulate the inference problem in document-level RE as a Masked Image Reconstruction (MIR) problem. Then, we propose an Inference Multi-head Self-Attention (I-MSA) module to restore masked images more efficiently. The MIR task and the I-MSA module greatly improve the inference ability of our model. Experiments on three public document-level RE datasets demonstrate that our DRE-MIR model achieved better results than the existing

state-of-the-art model. In the future, we will try to use our model for other inter-sentence or document-level tasks, such as cross-sentence collective event detection.

References

[Baldini Soares *et al.*, 2019] Livio Baldini Soares, Nicholas FitzGerald, Jeffrey Ling, and Tom Kwiatkowski. Matching the blanks: Distributional similarity for relation learning. In *Proc. of ACL*, 2019.

[Bao *et al.*, 2021] Hangbo Bao, Li Dong, and Furu Wei. Beit: Bert pre-training of image transformers. *arXiv preprint arXiv:2106.08254*, 2021.

[Beltagy *et al.*, 2019] Iz Beltagy, Kyle Lo, and Arman Cohan. Scibert: A pretrained language model for scientific text. *arXiv preprint arXiv:1903.10676*, 2019.

[Christopoulou *et al.*, 2019] Fenia Christopoulou, Makoto Miwa, and Sophia Ananiadou. Connecting the dots: Document-level neural relation extraction with edge-oriented graphs. *arXiv preprint arXiv:1909.00228*, 2019.

[Devlin *et al.*, 2018] Jacob Devlin, Ming-Wei Chang, Kenton Lee, and Kristina Toutanova. Bert: Pre-training of deep bidirectional transformers for language understanding. *arXiv preprint arXiv:1810.04805*, 2018.

[Goyal *et al.*, 2017] Priya Goyal, Piotr Dollár, Ross Girshick, Pieter Noordhuis, Lukasz Wesolowski, Aapo Kyrola, Andrew Tulloch, Yangqing Jia, and Kaiming He. Accurate, large minibatch sgd: Training imagenet in 1 hour. *arXiv preprint arXiv:1706.02677*, 2017.

[Guo *et al.*, 2019] Zhijiang Guo, Yan Zhang, and Wei Lu. Attention guided graph convolutional networks for relation extraction. *arXiv preprint arXiv:1906.07510*, 2019.

[He *et al.*, 2021] Kaiming He, Xinlei Chen, Saining Xie, Yanghao Li, Piotr Dollár, and Ross Girshick. Masked autoencoders are scalable vision learners. *arXiv preprint arXiv:2111.06377*, 2021.

[Huang *et al.*, 2017] Gao Huang, Zhuang Liu, Laurens Van Der Maaten, and Kilian Q Weinberger. Densely connected convolutional networks. In *Proc. of CVPR*, 2017.

[Jia *et al.*, 2019] Robin Jia, Cliff Wong, and Hoifung Poon. Document-level n -ary relation extraction with multiscale representation learning. *arXiv preprint arXiv:1904.02347*, 2019.

[Kipf and Welling, 2016] Thomas N Kipf and Max Welling. Semi-supervised classification with graph convolutional networks. *arXiv preprint arXiv:1609.02907*, 2016.

[Li *et al.*, 2016] Jiao Li, Yueping Sun, Robin J Johnson, Daniela Sciaky, Chih-Hsuan Wei, Robert Leaman, Allan Peter Davis, Carolyn J Mattingly, Thomas C Wiegers, and Zhiyong Lu. Biocreative v cdr task corpus: a resource for chemical disease relation extraction. *Database*, 2016.

[Li *et al.*, 2020] Bo Li, Wei Ye, Zhonghao Sheng, Rui Xie, Xiangyu Xi, and Shikun Zhang. Graph enhanced dual attention network for document-level relation extraction. In *Proc. of COLING*, 2020.

[Loshchilov and Hutter, 2017] Ilya Loshchilov and Frank Hutter. Decoupled weight decay regularization. *arXiv preprint arXiv:1711.05101*, 2017.

[Nan *et al.*, 2020] Guoshun Nan, Zhijiang Guo, Ivan Sekulic, and Wei Lu. Reasoning with latent structure refinement for document-level relation extraction. In *Proc. of ACL*, 2020.

[Qiu *et al.*, 2019] Lin Qiu, Yunxuan Xiao, Yanru Qu, Hao Zhou, Lei Li, Weinan Zhang, and Yong Yu. Dynamically fused graph network for multi-hop reasoning. In *Proc. of ACL*, 2019.

[Quirk and Poon, 2016] Chris Quirk and Hoifung Poon. Distant supervision for relation extraction beyond the sentence boundary. *arXiv preprint arXiv:1609.04873*, 2016.

[Ramesh *et al.*, 2021] Aditya Ramesh, Mikhail Pavlov, Gabriel Goh, Scott Gray, Chelsea Voss, Alec Radford, Mark Chen, and Ilya Sutskever. Zero-shot text-to-image generation. *arXiv preprint arXiv:2102.12092*, 2021.

[Ronneberger *et al.*, 2015] Olaf Ronneberger, Philipp Fischer, and Thomas Brox. U-net: Convolutional networks for biomedical image segmentation. In *International Conference on Medical image computing and computer-assisted intervention*, 2015.

[Schlichtkrull *et al.*, 2018] Michael Schlichtkrull, Thomas N Kipf, Peter Bloem, Rianne Van Den Berg, Ivan Titov, and Max Welling. Modeling relational data with graph convolutional networks. In *European semantic web conference*, 2018.

[Tang *et al.*, 2020] Hengzhu Tang, Yanan Cao, Zhenyu Zhang, Jiangxia Cao, Fang Fang, Shi Wang, and Pengfei Yin. Hin: Hierarchical inference network for document-level relation extraction. *Advances in Knowledge Discovery and Data Mining*, 2020.

[Veličković *et al.*, 2017] Petar Veličković, Guillem Cucurull, Arantxa Casanova, Adriana Romero, Pietro Lio, and Yoshua Bengio. Graph attention networks. *arXiv preprint arXiv:1710.10903*, 2017.

[Verga *et al.*, 2018] Patrick Verga, Emma Strubell, and Andrew McCallum. Simultaneously self-attending to all mentions for full-abstract biological relation extraction. In *Proc. of ACL*, 2018.

[Wang *et al.*, 2019] Hong Wang, Christfried Focke, Rob Sylvester, Nilesh Mishra, and William Wang. Fine-tune bert for docred with two-step process. *arXiv preprint arXiv:1909.11898*, 2019.

[Wang *et al.*, 2020] Difeng Wang, Wei Hu, Ermei Cao, and Weijian Sun. Global-to-local neural networks for document-level relation extraction. *arXiv preprint arXiv:2009.10359*, 2020.

[Wolf *et al.*, 2019] Thomas Wolf, Lysandre Debut, Victor Sanh, Julien Chaumond, Clement Delangue, Anthony Moi, Pierrick Cistac, Tim Rault, Rémi Louf, Morgan Funtowicz, et al. Huggingface’s transformers: State-of-the-art natural language processing. *arXiv preprint arXiv:1910.03771*, 2019.

[Wu *et al.*, 2019] Ye Wu, Ruibang Luo, Henry CM Leung, Hing-Fung Ting, and Tak-Wah Lam. Renet: A deep learning approach for extracting gene-disease associations from literature. In *Proc. of RECOMB*, 2019.

[Xu *et al.*, 2021a] Benfeng Xu, Quan Wang, Yajuan Lyu, Yong Zhu, and Zhendong Mao. Entity structure within and throughout: Modeling mention dependencies for document-level relation extraction. *arXiv preprint arXiv:2102.10249*, 2021.

[Xu *et al.*, 2021b] Wang Xu, Kehai Chen, and Tiejun Zhao. Document-level relation extraction with reconstruction. In *Proc. of AAAI*, 2021.

[Yao *et al.*, 2019] Yuan Yao, Deming Ye, Peng Li, Xu Han, Yankai Lin, Zhenghao Liu, Zhiyuan Liu, Lixin Huang, Jie Zhou, and Maosong Sun. DocRED: A large-scale document-level relation extraction dataset. In *Proc. of ACL*, 2019.

[Ye *et al.*, 2020] Deming Ye, Yankai Lin, Jiaju Du, Zhenghao Liu, Peng Li, Maosong Sun, and Zhiyuan Liu. Coreferential reasoning learning for language representation. *arXiv preprint arXiv:2004.06870*, 2020.

[Zeng *et al.*, 2015] Daojian Zeng, Kang Liu, Yubo Chen, and Jun Zhao. Distant supervision for relation extraction via piecewise convolutional neural networks. In *Proc. of EMNLP*, 2015.

[Zeng *et al.*, 2020] Shuang Zeng, Runxin Xu, Baobao Chang, and Lei Li. Double graph based reasoning for document-level relation extraction. In *Proc. of EMNLP*, 2020.

[Zeng *et al.*, 2021] Shuang Zeng, Yuting Wu, and Baobao Chang. Sire: Separate intra-and inter-sentential reasoning for document-level relation extraction. *arXiv preprint arXiv:2106.01709*, 2021.

[Zhang *et al.*, 2018] Yuhao Zhang, Peng Qi, and Christopher D. Manning. Graph convolution over pruned dependency trees improves relation extraction. In *Proc. of EMNLP*, 2018.

[Zhang *et al.*, 2020] Zhenyu Zhang, Bowen Yu, Xiaobo Shu, Tingwen Liu, Hengzhu Tang, Wang Yubin, and Li Guo. Document-level relation extraction with dual-tier heterogeneous graph. In *Proc. of COLING*, 2020.

[Zhang *et al.*, 2021a] Ningyu Zhang, Xiang Chen, Xin Xie, Shumin Deng, Chuanqi Tan, Mosha Chen, Fei Huang, Luo Si, and Huajun Chen. Document-level relation extraction as semantic segmentation. *arXiv preprint arXiv:2106.03618*, 2021.

[Zhang *et al.*, 2021b] Ningyu Zhang, Qianghuai Jia, Shumin Deng, Xiang Chen, Hongbin Ye, Hui Chen, Huaixiao Tou, Gang Huang, Zhao Wang, Nengwei Hua, et al. Alicg: Fine-grained and evolvable conceptual graph construction for semantic search at alibaba. *arXiv preprint arXiv:2106.01686*, 2021.

[Zhang *et al.*, 2021c] Shengyu Zhang, Dong Yao, Zhou Zhao, Tat-Seng Chua, and Fei Wu. Causerec: Counterfactual user sequence synthesis for sequential recommendation. In *Proc. of SIGIR*, 2021.

[Zhong and Chen, 2020] Zexuan Zhong and Danqi Chen. A frustratingly easy approach for entity and relation extraction. *arXiv preprint arXiv:2010.12812*, 2020.

[Zhou and Chen, 2021] Wenxuan Zhou and Muhaoo Chen. An improved baseline for sentence-level relation extraction. *arXiv preprint arXiv:2102.01373*, 2021.

[Zhou *et al.*, 2020] Huiwei Zhou, Yibin Xu, Weihong Yao, Zhe Liu, Chengkun Lang, and Haibin Jiang. Global context-enhanced graph convolutional networks for document-level relation extraction. In *Proc. of COLING*, 2020.

[Zhou *et al.*, 2021a] Jinghao Zhou, Chen Wei, Huiyu Wang, Wei Shen, Cihang Xie, Alan Yuille, and Tao Kong. ibot: Image bert pre-training with online tokenizer. *arXiv preprint arXiv:2111.07832*, 2021.

[Zhou *et al.*, 2021b] Wenxuan Zhou, Kevin Huang, Tengyu Ma, and Jing Huang. Document-level relation extraction with adaptive thresholding and localized context pooling. In *Proc. of AAAI*, 2021.

Dataset	DocRED	CDR	GDA
Train	3053	500	23353
Dev	1000	500	5839
Test	1000	500	1000
Relations	97	2	2
Entities per Doc	19.5	7.6	5.4
Mentions per Doc	26.2	19.2	18.5
Entities per Sent	3.58	2.48	2.28

Table 6: Summary of DocRED, CDR and GDA datasets.

Hyperparam	DocRED BERT	CDR SciBERT	GDA SciBERT
Batch size	8	16	16
Epoch	100	20	5
lr for encoder	2e-5	2e-5	2e-5
lr for other parts	1e-4	5e-5	5e-5

Table 7: Hyper-parameters Setting.

A Datasets

Table 5 details the statistics of the three document-level relational extraction datasets, DocRED, CDR, and GDA. These statistics further demonstrate the complexity of entity structure in document-level relation extraction tasks.

B Hyper-parameters Setting

Table 6 details our hyper-parameters setting. All of our hyper-parameters were tuned on the development set.